This manuscript was published as formal in:

Carbohydrate Polymers Volume 152, 5 November 2016, Pages 306-316

https://doi.org/10.1016/j.carbpol.2016.07.007

https://www.sciencedirect.com/science/article/pii/S0144861716307962

Title:

Dual crosslinked iminoboronate-chitosan hydrogels with strong antifungal activity against *Candida* planktonic yeasts and biofilms

by:

Daniela Ailincai[a], Luminita Marin[a], Simona Morariu[a], Mihai Mares[b], Andra-Cristina Bostanaru[b], Mariana Pinteala[a], Bogdan C. Simionescu[a,c], Mihai Barboiu[a,d]*

[a]"Petru Poni" Institute of Macromolecular Chemistry of Romanian Academy – 41A, Aleea Gr. Ghica Voda, Iasi, Romania

[b]"Ion Ionescu de la Brad" University, Laboratory of Antimicrobial Chemotherapy, 8, Aleea Sadoveanu, Iasi, Romania

[c]"Gheorghe Asachi" Technical University of Iasi – 73, Bd. Dimitrie Mangeron, Iasi, Romania

[d]Institut Européen des Membranes – F-34095, Place Eugène Bataillon, Montpellier, France

*Corresponding Author Luminita Marin

e-mail: lmarin@icmpp.ro

Abstract

Chitosan based hydrogels are a class of cross-linked materials intensely studied for their biomedical, industrial and environmental application, but their biomedical use is limited because of the toxicity of different organic crosslinkers. To overcome this disadvantage, a new strategy to produce supramolecular chitosan hydrogels using low molecular weight compounds able to form covalent linkages and H-bonds to give a dual crosslinking is proposed. For this purpose we used 2-formylphenylboronic acid, which brings the advantage of imine stabilization *via* iminoboronate formation and potential antifungal activity due to the presence of boric acid residue. FTIR and NMR spectroscopy indicated that the gelling process took place by chemo-physical crosslinking forming a dual iminoboronate-chitosan network. Further, X-ray diffraction demonstrated a three-dimensional nanostructuring of the iminoboronate network with consequences on the micrometer-scale morphology and on the improvement of mechanical properties, as demonstrated by SEM and rheological investigation. The hydrogels proved strong antifungal activity against *Candida* planktonic yeasts and biofilms, promising to be a friendly treatment of the recurrent vulvovaginitis infections.

Keywords: hydrogels, iminoboronate, chitosan, supramolecular, antifungal, rheology

1. Introduction

Hydrogels are three-dimensional polymeric networks which are able to hold a large amount of water or biological fluids, with applicability in a high number of biomedical, industrial and environmental purposes starting with drug delivery, wound dressing, soft contact lenses or diapers, as well as in restorative dentistry, tissue engineering, water waste treatment and soil conditioning (Buenger, Topuz & Groll, 2012; Chawla, Ranjan Srivastava, Pandey & Chawla, 2014; Ullah et al., 2015). Many polymers proved the ability to form

hydrogels, in the presence or absence of a crosslinking agent (Palumbo et al., 2015). Among them, chitosan, the second most abundant natural polymer, is recognised as an excellent option due to its rich therapeutic properties: biocompatibility and biodegradability, hemostatic, hypolipidemic, hypoglycemic, antitumoral, antimicrobial and fungicidal activity – to mention only some (Ravi Kumar M.N.V., Muzzarelli R.A.A., Muzzarelli C., Sashiwa & Domb, 2004; Muzzarelli R.A.A., 2009). Chitosan based hydrogels can be obtained by either physical or chemical crosslinking. The physically crosslinked chitosan hydrogels present the advantage of being temperature responsive, but their application is limited due to their weak mechanical properties and uncontrolled dissolution (Bhattarai, Gunn & Zhang, 2010). The chemically crosslinked chitosan hydrogels show slower degradability and possibility to control their pore size being recommended for *in vivo* long-term applications (Beauchamp, St Clair, Fennell, Clarke & Morgan, 1992). Some attempts to combine the two crosslinking ways resulted in dual-network hydrogels with improved mechanical properties, promising to be a reliable route to high performance materials (Fajardo, Favaro, Rubira & Muniz, 2013; Bai et al., 2016).

Since chitosan is a polysaccharide which contains functional amine groups, the primary pathway of its crosslinking is the acid condensation with dialdehydes, especially glutaraldehyde, forming imine bonds. Due to the reversibility of the imine bond formation, the obtained hydrogels have the advantage of being pH-responsive and biodegradable (Mi, Kuan, Shyu, Lee & Chang, 2000). Nevertheless, the toxicity of dialdehydes, and especially of glutaraldehyde, related to the human body restricts their use for biomedical applications (Beauchamp et al., 1992; Berger et al., 2004) and imposes the necessity to find new friendly crosslinking agents. Thus, the preparation of hydrogels with impact in the biomedical field remains a challenge of current interest (Berger et al., 2004; Mahkam, 2010; Azevedo & Kumar V., 2012; Mikhailov et al., 2016).

In finding a pathway toward hydrogels for biomedical applications, we propose the use of 2-formylphenylboronic acid as chitosan crosslinker, based on the assumption that its structure should facilitate a dual crosslinking – a covalent one *via* imine forming and a physical one *via* H-bonding, giving rise to a chemo-physical chitosan network. Additionally, due to the *ortho* position of the boric acid residue, the further stabilization of the imine linkage through intra-molecular H-bonds or dative linkages *via* an iminoboronate motif is possible. Recently considered as a powerful tool for bio-orthogonal dynamic covalent chemistry, the iminoboronates proved the ability to specifically target lipids, peptides and proteins as well as cancer-cells (Bandyopadhyay, McCarthy, Kelly & Gao, 2015; Cal et al., 2014). The dynamic iminoboronate unit may allow the reorganization and the adaptation in response to various external stimuli like pH or temperature, creating materials for new applications in biotechnology and medicine. On the other hand, considering the anticancer activity of boronic-imine compounds, and their low toxicity [Pasa et al., 2016] and the antifungal activity of the boric acid in the treatment of recurrent and resistant yeast vaginitis (De Seta, Schmidt, Vu, Essmann & Larsen, 2009), it is expected that the combination of 2-formylphenylboronic acid with chitosan to create novel products with improved biological activity.

In this paper, we present a novel synthetic strategy to develop chitosan based hydrogels using 2-formylphenylboronic acid as a dual crosslinking agent. The chemical and supramolecular structure of the iminoboronate-chitosan hydrogels, their morphology, rheological behaviour, swelling ratio, as well as antifungal activity against both planktonic and biofilm *Candida* yeasts were evaluated and discussed. Three novel aspects brought by the paper must be highlighted here: (i) the obtaining of iminoboronate derivatives of chitosan, (ii) the chitosan double crosslinking to give chemo-physical hydrogels, and (iii) the strong antifungal activity of the obtained hydrogels.

2. Experimental part

2.1 Materials

2-Formylphenylboronic acid (2-FPBA) (95%), low molecular weight chitosan (263 kDa, DA: 83%), D-glucosamine hydrochloride and phosphate buffer solution have been purchased from Aldrich and used without further purification. All the reagents used in antifungal measurements – Yeast Peptone Dextrose Agar (YPD), RPMI-1640, 3-(N-morpholino)propanesulfonic acid (MOPS), 2,3-bis(2-methoxy-4-nitro-5-sulfo-phenyl)-2H-tetrazolium-5-carboxanilide sodium salt (XTT), menadione, calcofluor (Fluorescent Brightener 28) – were purchased from Sigma-Aldrich and used as received.

2.2 General procedure for hydrogel and xerogel obtaining

To a 2% solution (g/mL) of chitosan (0.06 g, 0.29 mmol of glucosamine repeating units) in acidic water (0.7% acetic acid solution: 21 µL of acetic acid in 3mL of water) was added drop wise a 1% solution (g/mL) of 2-formylphenylboronic acid in ethanol (see Table 1), under vigorous magnetic stirring (500 rpm) at 55 ^{o}C. The molar ratio between NH_2 and CHO functional groups has been varied (keeping constant the amount of chitosan and changing the amount of aldehyde to achieve hydrogels with different crosslinking densities (see Table 1)). The reaction mixture reached the gelation point in less than 5 minutes for a NH_2 / CHO ratio of 1/1, and after 3 hours for the 2/1; 2.5/1; 3/1; 3.5/1; 3.75/1 ratios. No hydrogel has been obtained for the 4/1 molar ratio, the reaction mixture remaining a viscous liquid even after 24 hours. The visual examination revealed transparent semisolid materials with smooth texture, without air bubbles or other macroscopic particles. The hydrogels were kept uncovered for one day, up to the initial volume of chitosan solution was reached.

The corresponding xerogels of the obtained hydrogels were prepared by lyophilisation. As the NMR indicated the increase of the imine linkage density during a week, xerogels of the

hydrogels kept covered for one week, were also obtained. A 2% chitosan in 0.7 % acetic acid solution has been also lyophilized, to be used as a control reference. The codes of the hydrogels obtained for different molar ratios of the NH_2/CHO functional groups are given in table 1. Symbol * was used to designate the hydrogels kept one week before lyophilisation.

Table 1. The reaction parameters and codes of the understudy hydrogels

Code	**H0/ H0***	**H1/ H1***	**H2/H2***	**H2.5/ H2.5***	**H3/ H3***	**H3.5/ H3.5**	**H3.75/ H3.75***	**H4/ H4***
NH_2:CHO ratio	1:0	1:1	2:1	2.5:1	3:1	3.5:1	3.75:1	4:1
2-FPBA/g	-	0.045	0.023	0.018	0.015	0.013	0.012	0.011
2-FPBA/mmol	-	0.29	0.145	0.116	0.096	0.08	0.077	0.725
Ethanol/mL	-	4.5	2.3	1.8	1.5	1.3	1.2	1.1
Xerogel Weight/g	0.06	0.099	0.080	0.075	0.073	0.071	0.070	-
Yield %	100	99.62	99.51	99.85	99.77	99.78	99.7	-

2.3 Methods

The hydrogels were frozen in liquid nitrogen and further submitted to lyophilization using a Martin Christ, ALPHA 1-2LD equipment for 24 hours at -57 ºC and 0.050 mbar [Dinu, M. V., Pradny, M., Dragan, E. S. & Michalek, J., 2013].

FTIR spectra of the xerogels have been registered using a FT-IR Bruker Vertex 70 Spectrofotometer, by ATR technique and processed using OPUS 6.5 software.

The NMR spectra were obtained on a Bruker Avance DRX 400 MHz Spectrometer equipped with a 5 mm QNP direct detection probe and z-gradients. The chemical shifts are reported as δ values (ppm) relative to the residual peak of the deuterium oxide used as solvent.

Wide angle X-ray diffraction (WXRD) of the xerogel pellets was performed on a Bruker D8 Avance diffractometer with the Ni-filtered Cu-Kα radiation (λ = 0.1541 nm), in the range of 2-40° (2 theta degrees). The working conditions were 36 kV and 30 mA and data

were handled by the FullProf 2000 program. The xerogel pellets were obtained in a manual Hydraulic Press, by applying a pressure of 10 N/m^2.

The xerogel morphology was studied with a field emission Scanning Electron Microscope SEM EDAX – Quanta 200 at accelerated electron energy of 12.5 or 20 KeV.

Rheological tests were carried out at 37 °C by using a Bohlin CVO rheometer with a parallel plate geometry (60 mm diameter and 500 μm gap) and thermal control by the Peltier effect in closed system. An exhaustive description of the measurements is given in supporting information file.

Time-kill studies were performed using a previously described method (Canton, Peman, Gobernado, Viudes & Espinel-Ingroff, 2004), slightly modified as follows. A synthetic vagina-simulative medium (SVSM) was prepared (Moosa, Sobel, Elhalis, Du & Akins, 2004; Marques, Loebenberg & Almukainzi, 2011) to assure biomimetic conditions. Two clinical isolates *Candida albicans* RTCC 1112 and *Candida glabrata* RTCC 1532 were used as testing microorganisms (RTCC: Romanian Type Culture Collection). From each strain, a 5 McFarland suspension in SVSM was prepared and adjusted to 2.5 x 10^7 CFU/mL using the TC20 automated cell counter (Bio-rad, USA). Subsequently, equal volumes of yeast suspension and hydrogel solution in SVSM were mixed and incubated at 36±1°C, to obtain final mixtures with 2-FPBA concentrations of 0.142% and 0.071%, respectively. A drug free control was also prepared by mixing equal volumes of yeast suspension and SVSM. At predetermined time intervals (0, 6, 12 and 24 hours), a 1 mL aliquot from each test and control tube was serially diluted in sterile water, plated onto YPD, and incubated 48 hours at 36±1°C in order to evaluate the number of CFU/mL. The reproducible detection limit for colony counts is 10^1 CFU/mL.

The biofilms were obtained using the method described by Pierce (2008). To do the experiments, stock cultures of every isolate were resuscitated on Sabouraud Dextrose Agar

plates, for 24 to 48 h, at 37°C. Erlenmeyer flasks, with a capacity of 100 mL and containing 20 mL of Yeast Peptone Dextrose broth, were inoculated with one loopful of biomass from the stock cultures. The flasks were incubated overnight in an orbital shaker, at 30°C and 170-180 rpm. The cells were then collected and washed three times with phosphate buffer saline (PBS) by successive centrifugations and resuspensions. The yeast biomass was further used to obtain the suspension in RPMI medium. The tests were carried out in 96 wells microtiter plates. Yeast suspensions in RPMI-1640 without sodium bicarbonate and buffered with MOPS were adjusted to a density of 1.0 x 10_6 CFU/mL and 100 µL were transferred in microtiter plate wells (18 wells per each strain were used as follows: 6 for drug free control, 6 for 0.284% 2-FPBA, and 6 for 0.142% 2-FPBA). Blank wells filled with distilled water were also prepared. The plates were incubated 24 h at 36±1°C and afterwards washed three times with sterile water (200 µL per well) in order to remove the planktonic and/or the non-adherent cells. After washing the biofilms, 100 µL fresh SVSM medium was pipetted into the control wells, while 100 µL SVSM containing the H1* hydrogel was added to the test wells. The plates were incubated 24 h at 36±1°C and washed twice with 200 µL sterile water per well.

To assess the metabolic activity of the biofilms, 200 µL of 0.05% 2,3-bis(2-methoxy-4-nitro-5-sulfo-phenyl)-2H-tetrazolium-5-carboxanilide sodium salt (XTT) in PBS with 1 µM menadione were added to half of the control and test wells (9 wells per strain), and the plates were covered in aluminium foil and dark-incubated for 3 hours at 36±1°C. During the incubation period the active biofilms metabolize XTT and produce a water-soluble formazan which can be spectrophotometrically measured at 490 nm. This method allows a good correlation between cellular population and the metabolic activity of the biofilms (Pierce et al., 2008). The absorbance of the XTT solution was measured using the microplate reader model 680 (Bio-rad, USA) and each value obtained for the test wells was compared with the

control absorbance to determine the percentage of the biofilm metabolic activity reduction after the treatment with the hydrogel.

To evaluate the biofilm structure and extension, the other half of the control and test wells (9 wells per strain) were stained with 200 µL 0.1% calcofluor for 30 minutes and visualized under inverted microscope using ZOE Fluorescent Cell Imager (Bio-Rad, USA).

3. Results and discussions

3.1 Design and synthesis

Chitosan based hydrogels have been prepared by using a carbonyl compound named 2-formylphenylboronic acid (**2-FPBA**) as crosslinking agent (Scheme 1a). The boronic and the aldehyde groups of **2-FPBA** create the premises of both chemical crosslinking – *via* imine bonds with the chitosan amine groups, and physical crosslinking – *via* hydrogen bonding of the OH groups of the boronic moieties, respectively. In this manner, the obtained hydrogels should combine the advantages of chemical and physical crosslinking. Targeting medical applications, the reaction was performed in water/ethanol mixture, both solvents being biocompatible and nontoxic. Hydrogels with different crosslinking densities were prepared using variable molar ratios between the chitosan amino groups and the aldehyde functionality of 2-FPBA (Table 1). When heated at 75 ^{o}C, the hydrogels crosslinked with a low amount of aldehyde (**H3**, **H3.5**, **H3***, **H3.5***) collapsed, while those with a higher amount of aldehyde (**H1**, **H2**, **H2.5**, **H1***, **H2***, **H2.5***) kept their integrity. According to the literature, this indicated the predominance of physical interactions into the hydrogels with low amount of **2-FPBA** and the predominance of chemical crosslinking in the case of the hydrogels with higher amount [Ebara et al., 2014].

To confirm the synthetic pathway and to understand better the driving force which led to hydrogels obtaining, a model compound, **M** has been synthesised by reacting **2-FPBA** with

D-glucosamine (Scheme 1b). Data regarding its synthesis and structural characterization are given in supporting information (see Fig. 1s and 2s of supporting material).

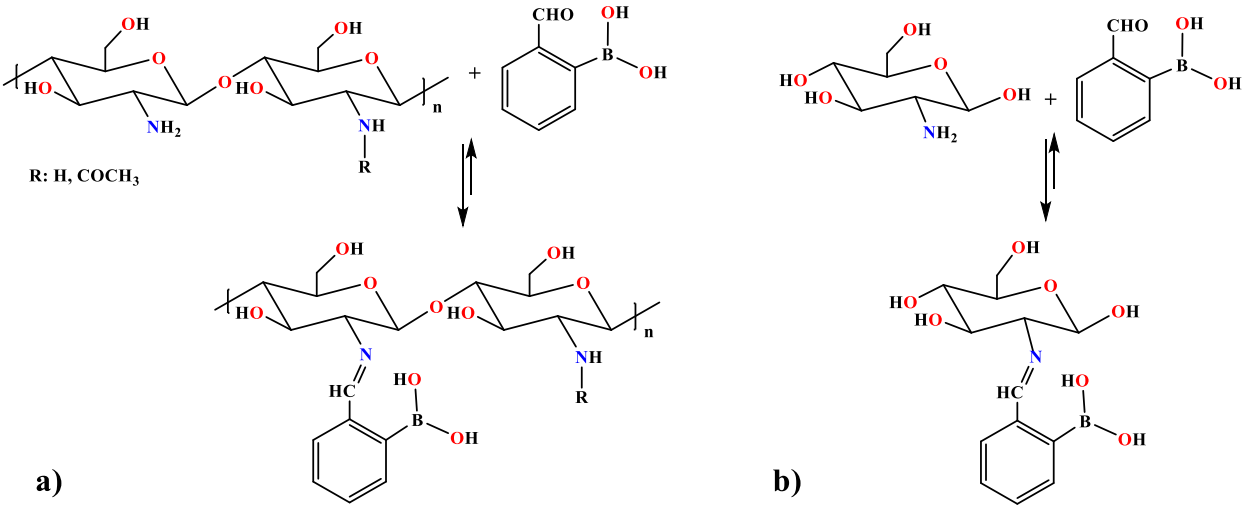

Scheme 1. The obtaining of the hydrogels and of the model compound

3.2 Structural characterization by FTIR spectroscopy

FTIR spectroscopy of the model compound and of the hydrogels has been employed as a sensible method which brings qualitative insights regarding the newly formed linkages, both chemical and physical ones, in order to decipher the mechanism of hydrogel formation (Fig. 1).

The FTIR spectrum of the model compound, **M** clearly exhibited the appearance of a new absorption band in the fingerprint region, at 1624 cm $^{-1}$ – characteristic to the group stretching vibrations of the imine bond. This band also appeared in the spectra of the hydrogels confirming the chemical crosslinking *via* imine bond formation. Compared to the parent chitosan which presented in this region a large band of low intensity at 1640 cm $^{-1}$ – specific to the secondary amide stretching, the newly formed imine band could be clearly detected as a sharper band located at 1624 cm^{-1}. The band is sharper and more intense as the amount of the used crosslinker increased, fact which is rationally attributed to an enhanced

density of imine bonds in those cases. On the other hand, as the content of the aldehyde crosslinker into hydrogels increased, the broad band at 1556 cm^{-1} characteristic to the deformation vibration of the N-H linkage gradually diminished and concomitant, the sharper band at 1560 cm^{-1} specific to the in plane skeletal vibration of the C=C bonds of the **2-FPBA** increased in intensity – reflecting the increased amount of the crosslinker in the hydrogel as the amine functional groups were consummated. Furthermore, the xerogel spectra showed the other bands characteristic to the aromatic ring of the **2-FPBA** e.g. out-of-plane C-H bending vibration at 760 cm^{-1}; stretching C-H vibration at 3070 – 3059 cm^{-1}; in plane bending at 1208 cm^{-1} and out-of-plane bending at 760 cm^{-1} of the B-OH.

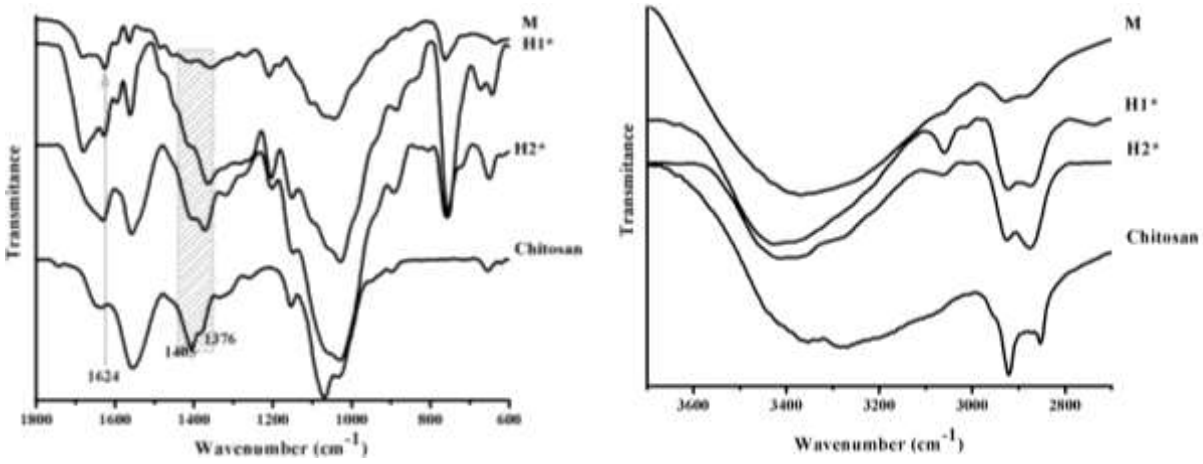

a) **b)**

Fig. 1. FTIR spectra of the hydrogels, **H1*** and **H2***, chitosan and model compound, **M**

Important information regarding the physical crosslinking has been brought by the changes produced in the 2700 – 3700 cm^{-1} domain of the hydrogel FTIR spectra compared to the parent chitosan (Fig. 1b). This spectral region has been demonstrated to be characteristic to the occurrence of stretching vibrations of the hydroxyl groups involved in hydrogen bonds, both intra- and inter-molecular (Marin et al., 2014). A broad halo, consisting in overlapped bands with two principal maxima located at 3362 and 3284 cm^{-1} attributed to the intra-molecular and inter-molecular H-bonds, respectively, appeared in the chitosan FTIR

spectrum. In the FTIR spectra of the hydrogels, the maximum attributed to the intra-molecular H-bonds (3362 cm^{-1}) is shifted to higher wavenumbers, in the range 3390 - 3430 cm^{-1}, as the crosslinker content increased, suggesting the appearance of new intra-molecular H-bonds. Considering the chemical structure of the newly formed imino-chitosan derivative, these new H-bonds could be mainly attributed to the intra-molecular H-bonds between the labile hydrogen of boric acid residue and the electron rich nitrogen atom of the imine units (Adamczyk-WoŸniak et al., 2012). In this context, a stabilization of the newly formed imine linkage by BOH•••N intra-molecular H-bonds can be foreseen, giving rise to an iminoboronate unit.

A FTIR spectral region which brings information related to the chitosan morphology is the one between 1500 – 1200 cm^{-1} (Fig. 1a). In this domain occur the absorption bands characteristic to the CH_2 bending, which are substantial affected by the environment of the hydrogen bonds, both intra- and inter-molecular (Marin et al., 2014). Comparing the chitosan spectrum to those of hydrogels, significant changes could be observed. Thus, the chitosan spectrum exhibited an overlapped band with two maxima – a more intense maximum at 1405 cm^{-1} and a less intense one at 1376 cm^{-1}. On contrary, in the hydrogel spectra the maximum at 1376 cm^{-1} became more intense, while the maximum at 1405 cm^{-1} diminished in intensity, suggesting drastic rearrangements of the H-bonding environment. Since the chitosan morphology is dominated by the preponderant intra-molecular H-bonds because of the coiled conformation of the chitosan backbones in solution, the drastic modification in terms of shape and intensity of the CH_2 bending band in the hydrogels was attributed to the prevailing of the inter-molecular H-bonds produced by the re-orientation of the primary –OH groups in the most favourable positions. This hypothesis is in good agreement with the straightening of the chitosan chains produced by grafting rigid imines, forcing the chitosan to unfold.

All the FTIR data lead to the conclusion that covalent crosslinking of the chitosan *via* imine linkages occurred in the presence of the **2-FPBA**. The imine bond is stabilized by the intra-molecular H-bonds which further constrain the coiled chitosan backbones to adopt a straight conformation which facilitates intermolecular H-bonding. Thus, the chemical and physical linking facilitated the forming of an iminoboronate-chitosan network.

3.3 Structural characterization by NMR spectroscopy

To further confirm the chemical crosslinking of chitosan *via* imine linkages and to asses a chemical crosslinking degree, the NMR spectroscopy has been used as a quantitative method. The model compound exhibited two chemical shifts, a less intense one at 8.7 ppm and a much intense one at 8.5 ppm attributed to the proton of the imine linkage in sin- and anti- conformations (Gutiérrez-Moreno, Medrano & Yatsimirsky, 2012; Marin, Damaceanu & Timpu, 2009).

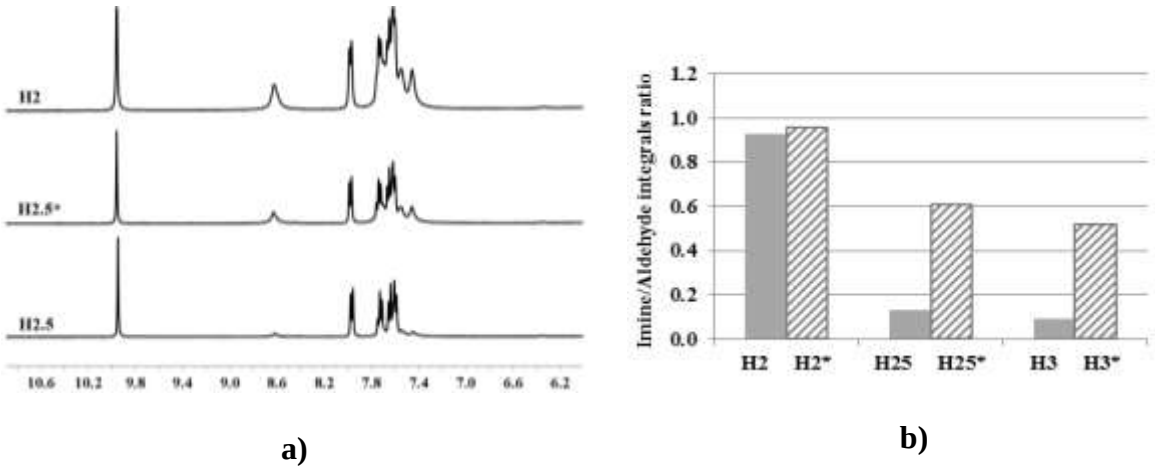

a) **b)**

Fig. 2. Representative NMR spectra (a) and graphical representation of the integral ratio of imine/aldehyde protons (b) of the hydrogels

The NMR spectra of the hydrogels exhibited the characteristic chemical shift of the imine proton at 8.6, 8.4 ppm, but also the chemical shift of the aldehyde proton at 9.94 ppm (Fig. 2a). Compared to the model compound, the intensity of the two singlet bands of the imine proton switched – the one at 8.6 ppm became very intense, while the one at 8.4 ppm almost disappeared, indicating the preponderant presence of one imine conformation. Taking

into consideration the chemical structure of the obtained iminoboronate-chitosan derivative, the preponderance of one imine conformation could be reached by the stabilization *via* a B-O-H•••N intra-molecular H-bond, which is favoured instead the N→B dative bond because of steric hindrance (Hutin, Bernardinelli & Nitschke, 2008; Adamczyk-WoŸniak et al., 2012). The integral ratio between the chemical shifts of the imine/aldehyde protons varies from 1/1 to 0.5/1, as the aldehyde content decreased, confirming a partial conversion degree of the **2-FPBA** into imine linkages, and thus a partial chemical crosslinking (Fig. 2b). It could be expected for the unreacted aldehyde to be employed in inter-molecular H-bonds, participating to a physical crosslinking. The NMR spectra registered from time to time, indicated that the integral ratio of the imine/aldehyde protons and thereby the degree of conversion of the aldehyde into imine linkages increased in the first week, indicating showing that the reaction equilibrium of the imine forming in water was reached in this time (see Fig. 3s of supporting material).

3.4 Supramolecular characterization by X-ray diffraction

In the light of the structural characterization by FTIR and NMR spectroscopy, the influence of the chemical crosslinking degree on the supramolecular architecture of the iminoboronate-chitosan network has been studied by wide angle X-ray diffraction measurements. As can be seen in fig. 3, the transforming of the chitosan poly-amine into a poly-iminoboronate network was accompanied by major changes of the packing peculiarities.

Chitosan exhibited a X-ray diffraction pattern typical for a semicrystalline polymer, exhibiting an overlapped band with two broad maxima around 12 and 21 °, characteristic to I and II crystallized phases. The large bands reflect the presence of orderly clusters of dried chitosan distributed into the amorphous state of hydrated chitosan. The broader and more intense peak at wider angle is the signature of the preponderant intramolecular hydrogen bonds (Leceta, Guerrero, Ibarburu, Dueñas & Caba, 2013). In the case of the understudy

iminoboronate-chitosan hydrogels, the broad halo from the 12 º disappeared and a new reflection band appeared around 6 º – consistent with a layered morphology (Baron, 2001). The band is missing for the hydrogels which were crosslinked with a lower amount of aldehyde and gets sharper and more intense while the aldehyde content increases related to a close relationship between the layered architecture and the density of covalent linkages. The corresponding inter-layer of 13.49 Å as calculated by Bragg law, met the inter-layer distance simulated by molecular mechanics MM+ for a straight conformation of the aromatic iminoboronate unit stabilized by intra-molecular H-bonds and a bilayer motif with antiparallel ordering of the imines of adjacent layers (Baron, 2001). Thus, the layering appeared to reflect a hydrophilic/hydrophobic segregation of the hydrophilic chitosan backbones and hydrophobic associations of aromatic imines, forming a supramolecular amphiphilic network, as shaped in fig. 3.

The broad reflection band around 20 º in the chitosan X-ray diffraction profile became sharper and is slightly shifted to smaller angles, around 21 º, in the X-ray diffractograms of the xerogels, corresponding to an inter-molecular distance of 4.39 Å, consistent with the inter-molecular distance between two pyranosic rings linked by inter-molecular H-bonds. The reflection is sharper as the content of aldehyde in the hydrogels increased, according to a modulated ordering (Baron, 2001) of the aromatic iminoboronate units forming crystalline clusters (Fig. 3).

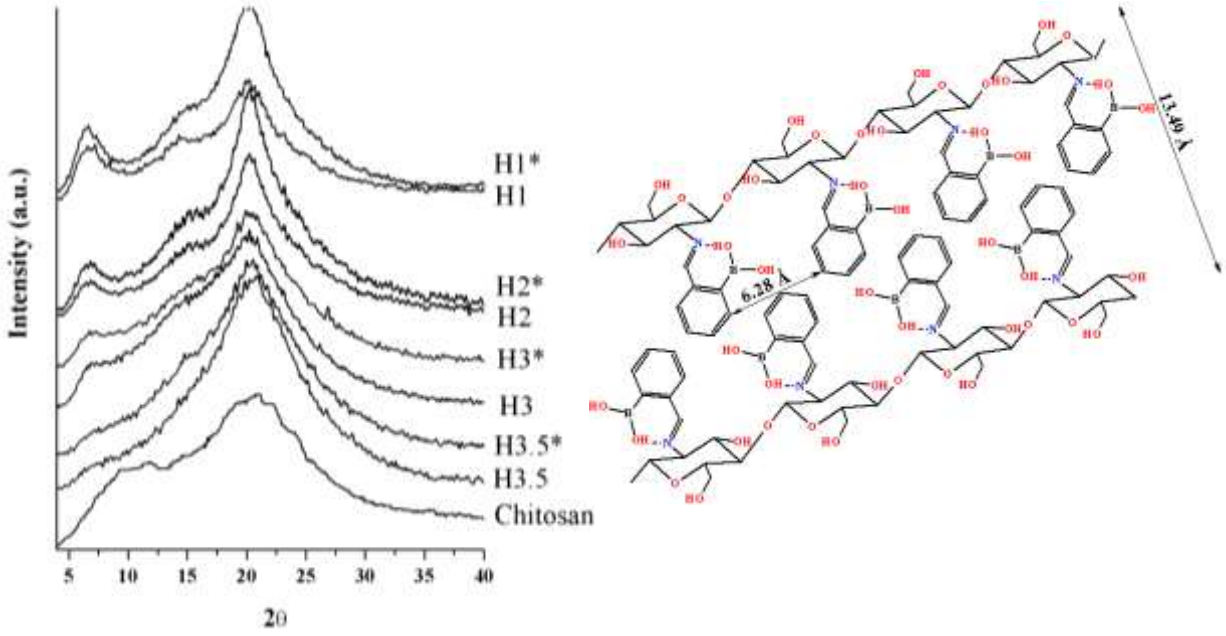

a) **b)**

Fig. 3. a) Representative X-ray diffraction of the iminoboronate-chitosan xerogels and chitosan reference; **b)** the schematic representation of an iminoboronate-chitosan cluster

Another particularity of the hydrogel X-ray pattern is the shifting of the medium angle band from 12 º in chitosan to 14.2 º in the hydrogels. The calculated distance of 6.28 Å is in agreement with the inter-molecular distance of 7.95 Å between two aromatic imines linked in neighbour positions on a chitosan chain. The reflection is more evident for the **H1**, **H2**, **H2.5** hydrogels based on predominant covalent bonds and disappeared for the **H3.5** hydrogel based on predominant physical bonds. Thus, it could be appreciated that nano-structuring of the hydrogels was close related to the forming of the covalent imine bonds.

The diffraction peaks became sharper and more intense in the case of the **H*** xerogels (kept 1 week before lyophilisation), especially for the hydrogels crosslinked with higher amount of **2-FPBA**. Correlating with the NMR data, this transformation was attributed to a structural reorganization due to imination and transimination processes (Marin, Simionescu & Barboiu, 2012; Marin et al., 2013; Marin et al., 2015). As a whole, the X-ray diffraction of the

hydrogels with higher content of **2-FPBA** is the expression of a three-dimensional ordering driven by the inter-layer, inter-molecular and inter-chain forces.

3.5 Hydrogel microstructure

As expected, the hydrogels have a highly porous interconnected morphology due to the large amount of water used in their obtaining (97 – 98%), forming a sponge-like microstructure (Fig. 4).

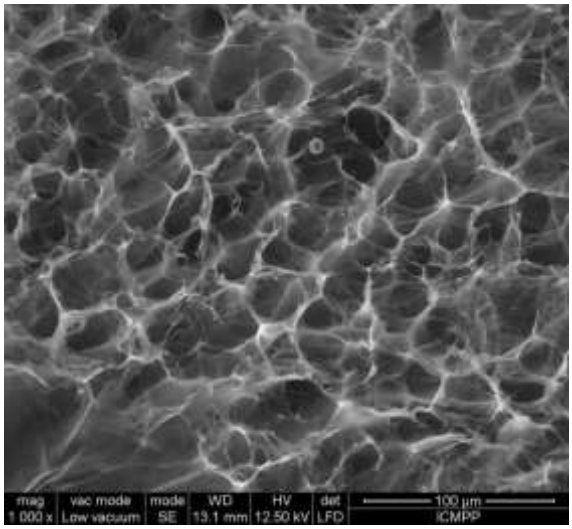

H2

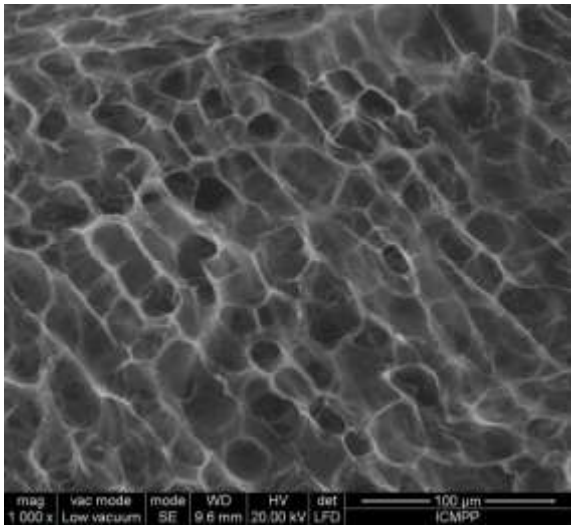

H2*

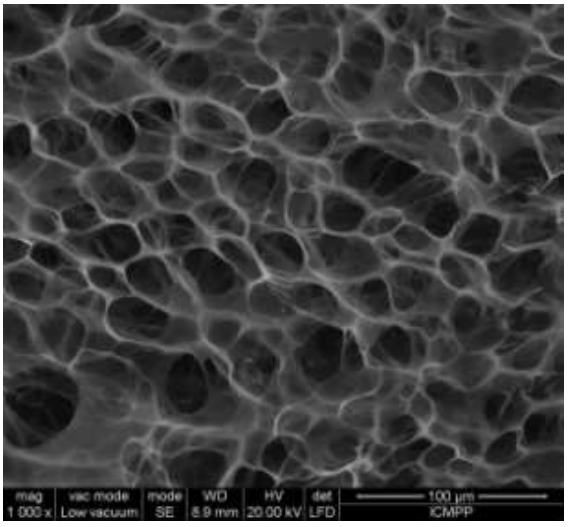

H3*

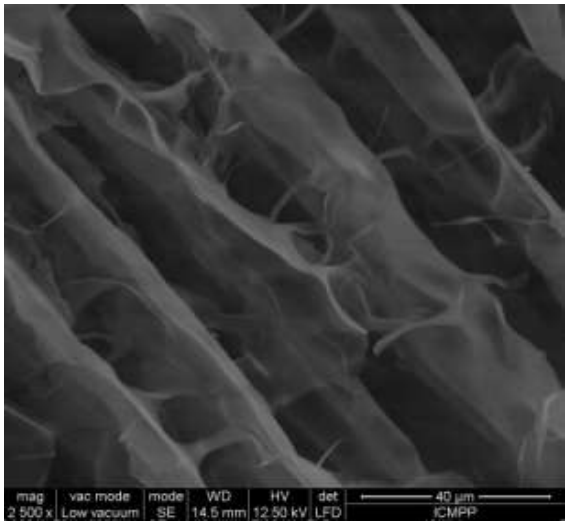

H3*

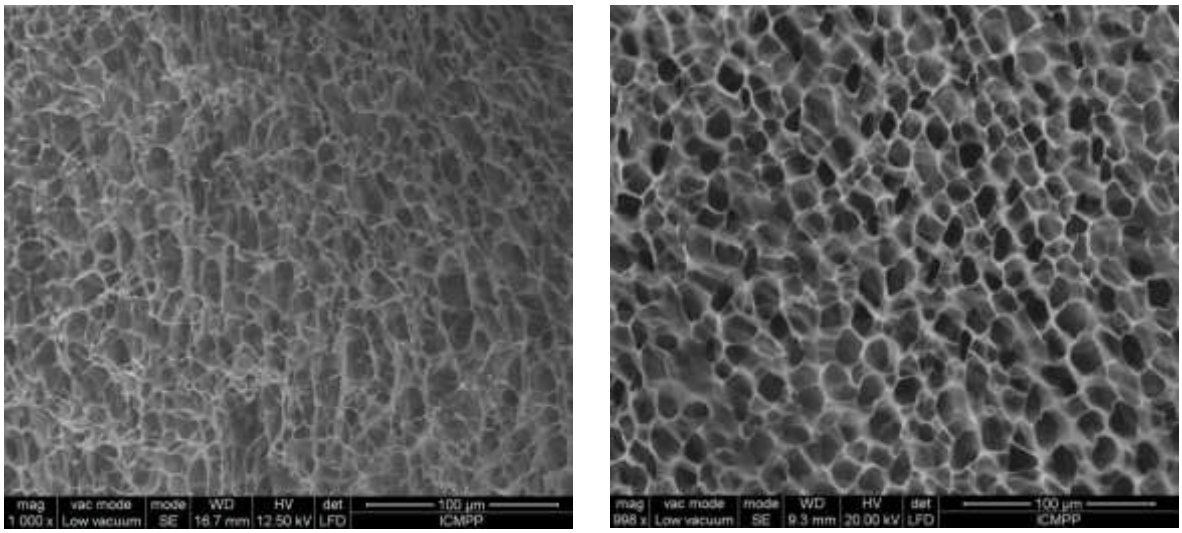

H3.5 **H3.5***

Fig. 4. Representative SEM images of the understudy hydrogels

The hydrogels obtained by using of a higher amount of **2-FPBA** showed a tighter microstructure with smaller inner pore size (see Fig. 4s of supporting material) due to the higher covalent crosslinking degree. Comparing the morphology of the (**H**) and (**H***) xerogels, one can observe a more homogeneous microstructure for the last ones, consisting in better defined pores with a more regular shape and a much narrower dimensional polydispersity, as can be seen from the obtained data for standard deviation (see Fig. 5s of supporting material).

3.6 Rheological investigation of the understudy hydrogels

The viscoelastic behaviour of the understudy hydrogels (H*), related to their nature and crosslinking density, was investigated at human body temperature of 37 ^{o}C. Storage modulus (G'), loss modulus (G''), apparent viscosity (η) and creep compliance (J) were evaluated by frequency sweep, continuous flow and creep-recovery tests for all the understudy hydrogels (Table 1s). Gel-like behaviour associated with the dominance of elastic component over the viscous one ($G' > G''$ ($tan\delta$ < 1)) was registered for crosslinking with higher amounts of aldehyde corresponding to the NH_2/CHO lower than 3.75 (Fig. 5a), while liquid-like behaviour was evidenced for **H4***, in agreement with the visual monitoring (Fig.

5b). Increasing the content of the aldehyde by changing the NH_2/CHO ratio from 3.75/1 to 2/1 was accompanied by an increase of G' and G'' with an order of magnitude, due to a higher crosslinking density of the chitosan chains.

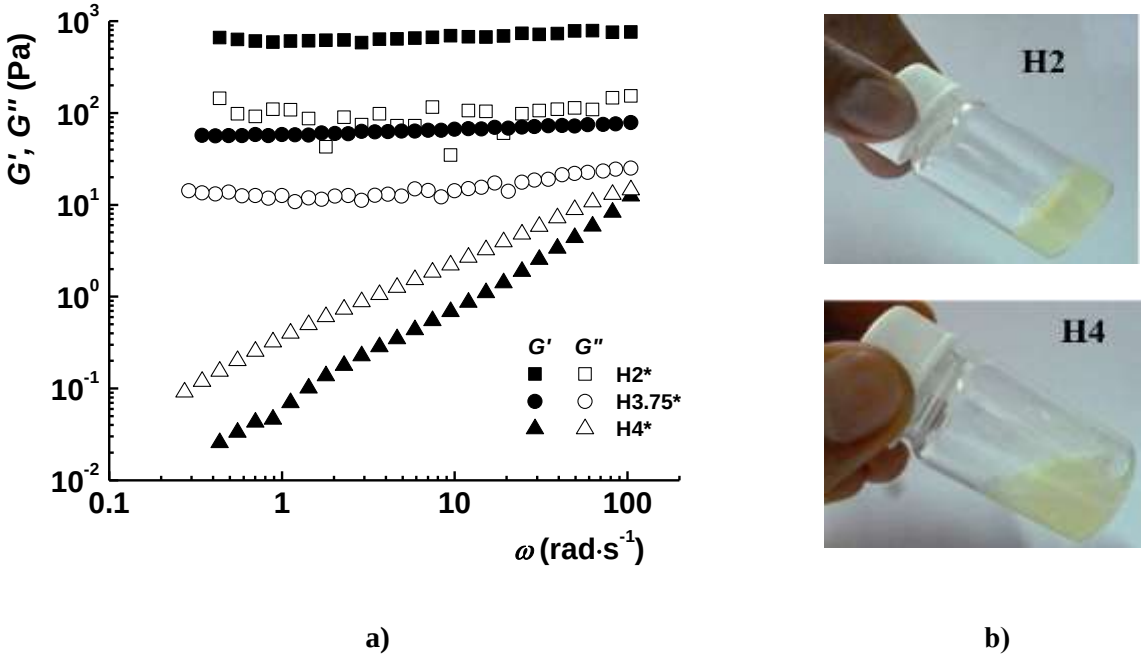

a) **b)**

Fig. 5. (a) Frequency dependence of G' and G'' for **H2***, **H3.75*** and **H4*** at 37 °C and 1 Pa and (b) pictures of two representative samples (H2*-gel like behaviour and H4*-liquid like behaviour)

Comparing the values of the G' elastic modulus of the hydrogels (Table 1s), it could be seen an upward trend with the increase of the amount of 2-**FPBA**, from 25 Pa (**H3.5**) to 648 Pa (**H2**), which was associated with a stiffening of the hydrogel network due to the increasing density of the imine covalent bonds.

An important aspect of the rheological behaviour of the hydrogels was related to the value of apparent viscosity. The investigations in continuous shear stress evidenced a decrease of the apparent viscosity (η) by increasing the shear rate ($\dot{\gamma}$), indicating a pseudoplastic behaviour for all the understudy hydrogels (Fig. 6a). The viscous sample **H4*** showed only a

slight decrease of the apparent viscosity, from about 0.35 Pas to 0.09 Pas by increasing the shear rate from 1.1 s^{-1} to 400 s^{-1} which is associated with a weak pseudoplastic behaviour. On the contrary, the hydrogel samples **H2*** – **H3.75*** exhibited an accentuated decrease of η during the increase of the shear rate above 0.01 s^{-1} attributed to the destruction of the orderly supramolecular architecture. The value of apparent viscosity at low shear rate suddenly decreased almost two orders of magnitude (from about 10^4 Pa s to 10^2 Pas) by reducing the content of **2-FPBA** from the **H3*** to **H3.5*** (inset of Fig. 6a) indicating that the collective strength of the structure was drastic reduced.

For a deeper insight upon the structure–crosslinking density relationship, the experimental data from the variation of apparent viscosity with shear rate were fitted with the simplified Carreau equation (Carreau, 1972). As can be seen in the inset of fig. 6a, the values of the zero shear viscosity imparted the hydrogels in three distinct types: (i) **H2***, **H2.5***, **H3*** characterized by the highest η_o values of 23 192 – 10 900 Pas; (ii) **H3.5*** and **H3.75*** characterized by η_o values drastically decreased around 500 Pas; and (iii) **H4*** characterized by η_o value of 0.35 Pas. The decreasing of the zero shear viscosity is in agreement with the assumption of supramolecular chemical hydrogels characterized by strong strength (**H2***, **H2.5***, **H3***) and physical hydrogels characterized by slighter stiffness (**H3.5***, **H3.75***). It appeared that the dramatic reduction of the structure strength is close related to the covalent crosslinking density which is the driving force of the formation of the supramolecular network.

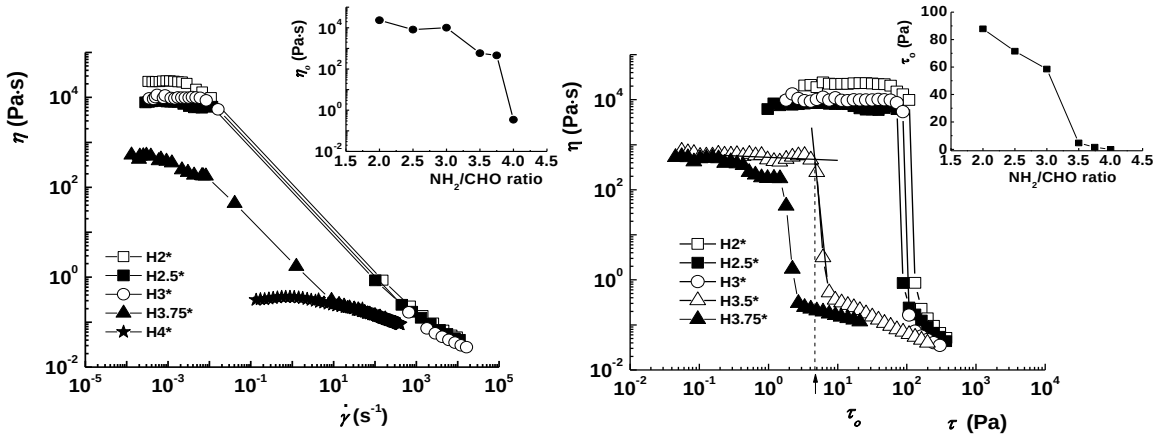

a) **b)**

Fig. 6. Variation of η as a function of (a) shear rate, $\dot{\gamma}$ and (b) shear stress, τ, for the understudy hydrogels, at 37 °C. The inset figures represent the effect of **2-FPBA** crosslinker amount on (a) η_o and (b) τ_o values, respectively

It is well known that the pseudoplastic materials show the variation of η as a function of the shear stress, τ: a constant apparent viscosity (η_o) up to a critical yield stress value, τ_o, when the viscosity abruptly decreases, meaning that the material starts to flow. Low values of the yield stress indicate an easier spreadability and a more difficult retention, important aspects for hydrogels applications in drug delivery or as scaffolds (Barners, 1999). Fig. 6b illustrates the variation of η as a function of τ values of the investigated samples. It can be observed that (i) **H4*** did not reveal any yield stress (see inset); (ii) **H3.75*** and **H3.5*** started to flow at a shear stress value lower than 5 Pa; and (iii) the yield stress of **H3***, **H2.5***, **H2*** increased at a threshold value around 90 Pa – indicating the hydrogels with lower content of aldehyde as the weakest and softest, and the hydrogels with higher content of aldehyde as the stiffest and strongest. In the variation of τ_o as a function of the **2-FPBA** crosslinker content, an abruptly decrease was evidenced at NH_2/CHO = 3 (inset of Fig. 6b), strengthening once more the idea of predominant physically or covalent crosslinking.

The time dependence of compliance for the studied samples is shown in Fig. 7. The samples **H2.5*** and **H3*** presented the lower J values indicating a stronger elastic structure which correlates well with the chemical supramolecular crosslinking of the chitosan *via* iminoboronate linkages. Opposite, the samples **H3.5***, **H3.75*** and **H4*** presented the higher J values characteristic to a less structured material.

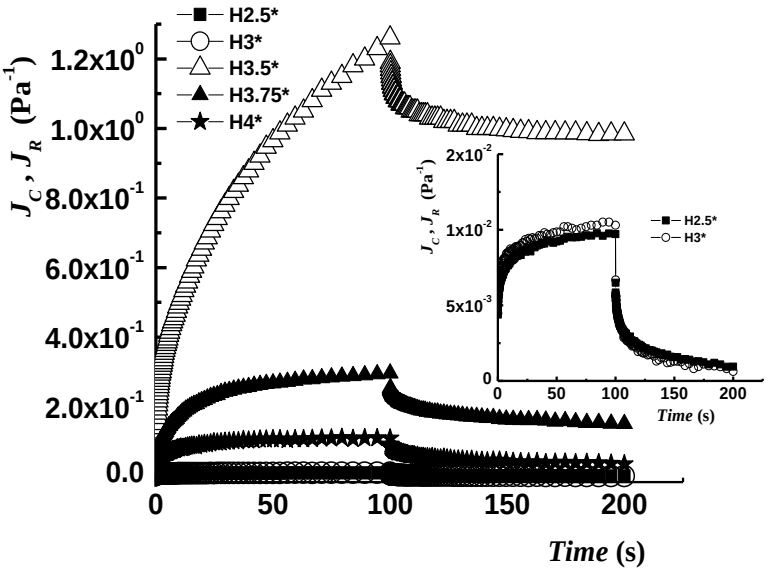

Fig. 7. Creep-recovery curves for **H2.5*** – **H4***, at 37 °C. The inset figure shows the creep-recovery curves for **H2.5*** and **H3***

The contribution of instantaneous elastic component, J_o and maximum compliance of Kelvin-Voigt element, J_{KV} to total deformation is roughly the same for all the investigated samples. The samples containing lower amounts of crosslinker (**H3.5***, **H3.75*** and **H4***), exhibited a lower contribution of the J_o and J_{KV} to total deformation, while the samples with a higher content of aldehyde (**H2.5*** and **H3***) exhibited a lower contribution of viscous component, J_∞ to deformation, indicating that the addition of a higher quantity of crosslinker increases the resistance of the hydrogels to the deformation. It appeared that the strong three-dimensional supramolecular network driven by the high density of covalent bonds (samples

H2.5* and **H3***) confers to the hydrogels the highest resistance to deformation, the forming of the spaced hydrophobic layers playing an important role.

The recovery degree decreases from about 90 % for **H2.5*** and **H3*** to 23.50 % for **H3.5*** (Table 3s). The high recovery degree of the samples crosslinked with a higher amount of aldehyde was attributed to the chemical supramolecular network which has the ability to break and restore under shear, in a similar manner to the liquid crystal mesophases.

The hydrogels swelled well reaching a MES value between 10 and 110, depending on their crosslinking degree and pH of the swelling solution (see Fig. 6s and corresponding discussions in supporting material).

3.7 Evaluation of the antifungal effect of iminoboronate hydrogels against planktonic yeast

The antifungal activity of the new iminoboronate-chitosan hydrogels was preliminary tested against *Candida albicans* and *Candida glabrata* strains – two virulent fungi accounting for systematic vulvovaginitis infections affecting the women's health (Sobel, 2016). As *Candida* strains have the ability to form pathogenic biofilm which is adherent to the host tissue, the antifungal activity was measured against planktonic strain growth and mature biofilm, respectively, in biomimetic conditions. To proper evaluate the antifungal activity, the measurements were carried out using the hydrogels and their pure components of similar concentration (Fig. 8a,b). The release kinetic of the **2-FPBA** from the hydrogels has been drawn too (Fig. 8c). It was observed that in the synthetic vagina-simulative medium, the hydrogel was able to prolong release the boronic aldehyde in the 24 hours of time testing, as a function of crosslinking type, in two steps: (i) firstly due to the easy breaking of the H-bonds, and (ii) secondly due to the iminoboronate forming reversibility (see supporting material).

Analysing the time-kill kinetics against the two studied *Candida* species (Fig. 8a,b) it could be observed that chitosan slows down the fungi growing comparing with the control

476 sample, proving weak inhibition effect. On the other hand, the pure aldehyde gradually killed
477 the *Candida* yeasts, which almost vanished in 24 hours, in the case of the concentration of
478 0.142 %. A similar trend could be identified in the case of the hydrogels, but with a slower
479 killing rate, according to the slower release of the aldehyde from the hydrogels. The kill-time
480 profile fit well with the release profile (Fig. 8).

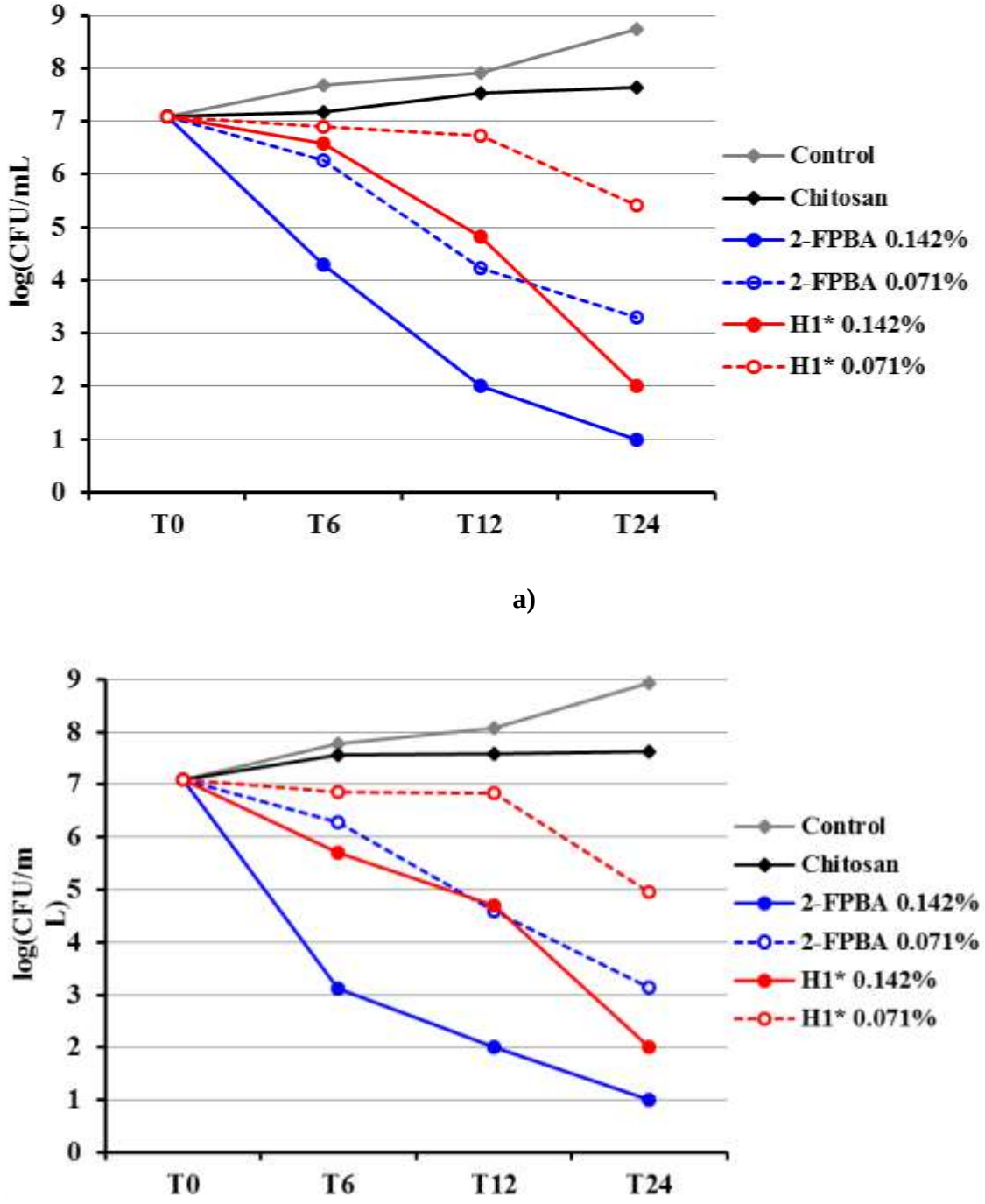

a)

b)

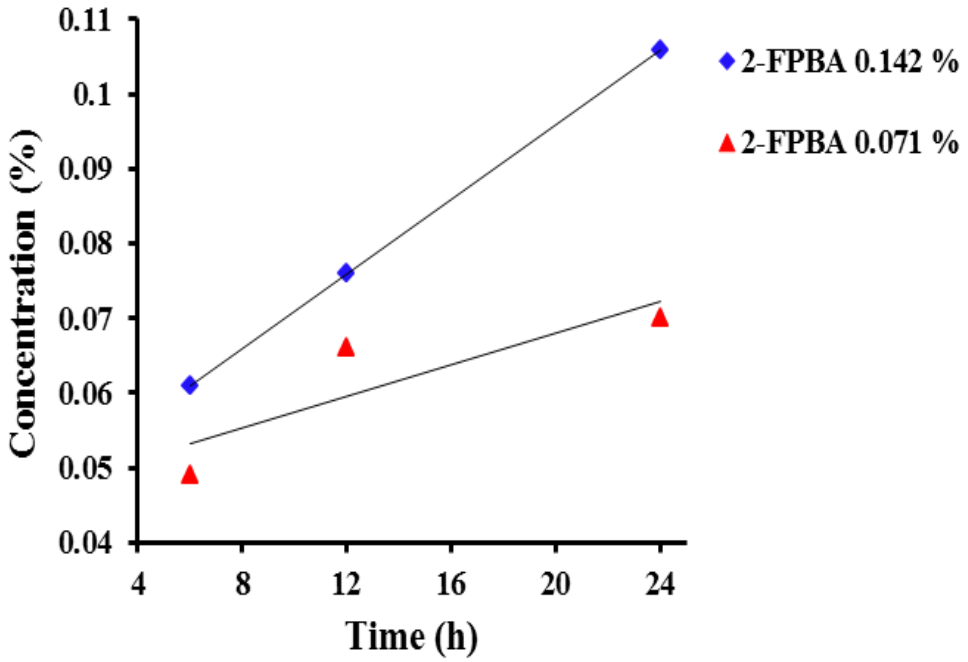

c)

Fig. 8. Evaluation of the fungicidal activity against planktonic yeast of a) *Candida albicans* and b) *Candida glabrata*; c) Release profile of the boronic aldehyde from the tested hydrogel

Corroborating data, it could be appreciated that the understudy hydrogels have a potent fungicidal effect against planktonic yeast belonging to *C. albicans* and *C. glabrata* species, at a concentration of 0.142 % of aldehyde in hydrogel, which appeared to be the most active concentration. Moreover, the microbial burden reduction exceeded 5log (99.999 % killing) after 24 hours, value that clearly surpasses the usual fungicidal endpoint (99.9% killing) (Canton et al., 2004; Lee et al., 2015).

3.9 Evaluation of the antifungal effect of iminoboronate hydrogels against yeast biofilms

Candida yeasts have the ability to form biofilms resistant to the penetration of antifungal agents, which further produce the recurrence of vaginitis. To investigate the ability of the understudy hydrogels not only to kill the planktonic yeast but also to disrupt an

494 eventual preformed biofilm, their activity against mature *Candida* biofilms was tested by
495 measuring biofilm metabolic reduction by spectrometry and analysis of biofilm structure
496 (Table 3) and extension under optical microscopy (Fig. 9). Being known that biofilm is much
497 more resistant compared to the planktonic films, two hydrogel concentrations (i) one
498 corresponding to a content of 0.142 % **2-FPBA** and (ii) another one of 0.284 % 2-**FPBA**
499 were considered.

500 The hydrogels strongly inhibited the formation of both yeast biofilms and their
501 metabolic activity at both concentrations. Their efficiency in biomimetic conditions was very
502 high, the metabolic activity of biofilms being reduced more than 99.5% *versus* less than 7% in
503 the case of 2% chitosan (Table 4s).

504 Comparing with non-treated biofilms that due to an important matrix production are
505 less structured, amorphous in appearance, the biofilms treated with hydrogels are "nude",
506 showing filamentous structure and lack of extracellular matrix (Fig. 9), consistent with an
507 inhibition mechanism by the blockage of the metabolic activity (Pierce et al., 2008).

508

509 **Table 3**. XTT assay – Decreasing of biofilm metabolic activity

Tested strains	Control	0.142% **2-FPBA** in **H1***		0.284% **2-FPBA** in **H1***	
	Abs ($\bar{x}$)	Abs ($\bar{x}$)	% reduction	Abs ($\bar{x}$)	% reduction
C. albicans 1112	0.758	0.002	99.74	0.001	99.87
C. glabrata 1532	1.020	0.007	99.31	0.003	99.71

510 Legend: Abs ($\bar{x}$) – absorbance arithmetic mean

511

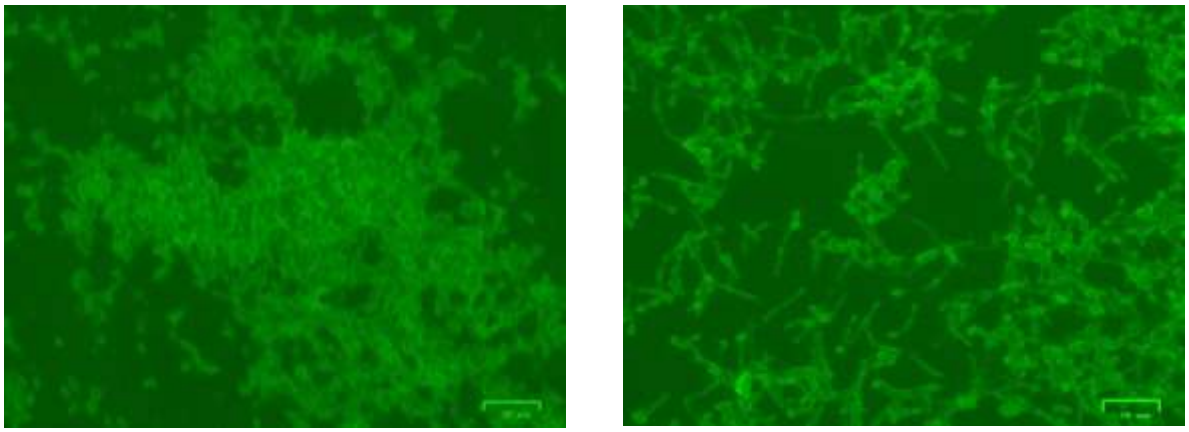

a) **b)**

Fig. 9. a) *C. albicans* mature biofilm in a drug-free control well after 48 hours: abundant matrix embedding the filaments and sessile yeast cells; **b)** *C. albicans* biofilm after the treatment with hydrogel containing 0.284% **2-FPBA**, for 24 hours: visible filaments and sessile yeast cells, matrix in trace amounts.

4. Conclusions

Iminoboronate-chitosan hydrogels were successfully prepared using 2-formyphenylboronic acid, **2-FPBA** as a low molecular weight dual cross-linker. By varying the molar ratio of the amine/aldehyde functionalities, hydrogels with different degrees of chemical/physical crosslinking have been obtained. The preponderant covalent hydrogels formed a supramolecular architecture with three-dimensional order based on the hydrophilic/ hydrophobic segregation of the hydrophilic chitosan and hydrophobic aromatic iminoboronate units. The hydrophobic layers appeared to be built according to a bilayer motif which improved the mechanical properties of the hydrogels. The rheological investigations demonstrated the predominant chemical hydrogels as very elastic structures, stiff and strong, with a high resistance to deformation and a recovery degree around 90 %. The hydrogels swelled well reaching a MES value between 10 and 110, depending on their crosslinking degree and on the pH of the swelling solution. They have efficient fungicidal activity in

biomimetic conditions against *Candida albicans* and *Candida glabrata* planktonic yeasts, at a low concentration, of 0.142 % of **2-FPBA** in hydrogel. Moreover, they inhibit the metabolic activity of the corresponding *Candida* biofilms more than 99.5 %, promising to be real candidates for the treatment of vulvovaginitis infections.

Supporting information

Experimental details regarding swelling and rheological measurements; Data for synthesis and characterization of model compound, **M**; NMR spectra of the understudy hydrogels; Tables containing rheological parameters; Representative histograms obtained using SEM images; Table and data related to the hydrogels swelling. This material is available free of charge via the Internet at http://pubs.acs.org.

Acknowledgements

The research leading to these results has received funding from the Romanian National Authority for Scientific Research, MEN – UEFISCDI grant, project number PN-II-RU-TE-2014-4-2314 and from Horizon 2020 ERA Chairs Project, no: 667387: SupraChemLab Laboratory of Supramolecular Chemistry for Adaptive Delivery Systems ERA Chair initiative.

References

Adamczyk-WoŸniak, A., Cyrański, M. K., Frączak, B. T., Lewandowska, A., Madura, I. D., Sporzyński, A. (2012) Imino- and aminomethylphenylboronic acids: stabilizing effect of hydrogen bonds. *Tetrahedron*, *68*, 3761–3767.

553 Azevedo, E.P. & Kumar V. (2012) Rheological, water uptake and controlled release
554 properties of a novel self-gelling aldehyde functionalized chitosan. *Carbohydrate*
555 *Polymers, 90*(2), 894– 900.
556 Bai, X., Lu, S., Cao, Z., Gao, C., Duan, H., Xu, X., Sun, L., Lao, N., Feng, C. & Liu, M.
557 (2016) Self-reinforcing injectable hydrogel with both high water content and mechanical
558 strength for bone repair. *Chemical Engineering Journal, 288*, 546-556.
559 Bandyopadhyay, A., McCarthy, K.A., Kelly, M.A. & Gao, J. (2015) Targeting bacteria via
560 iminoboronate chemistry of amine-presenting lipids. *Nature Communications*, *6,* 6561
561 Barners, H. A. (1999) A brief history of the yield stress. *Applied Rheology*, *9*(6), 262-266.
562 Baron, M. (2001) Definitions of basic terms relating to low-molar-mass and polymer liquid
563 crystals. *Pure and Applied Chemistry, 73*(5), 845-895.
564 Beauchamp, R.O., St Clair, M.B., Fennell, T.R., Clarke, D.O. & Morgan, K.T. (1992) A
565 critical review of the toxicology of glutaraldehyde. *Critical Reviews in Toxicology*, *22*(3-
566 4),143–174.
567 Berger, J., Reist, M., Mayer, J.M., Felt, O., Peppas, N.A. & Gurny, R. (2004) Structure and
568 interactions in covalently and ionically crosslinked chitosan hydrogels for biomedical
569 applications. *European Journal of Pharmaceutics and Biopharmaceutics*, *57*(1), 19-34.
570 Bhattarai, N., Gunn, J. & Zhang, M. (2010) Chitosan-based hydrogels for controlled,
571 localized drug delivery. *Advanced Drug Delivery Reviews*, *62*(1), 83-99.
572 Buenger, D., Topuz, F. & Groll, J. (2012) Hydrogels in sensing applications. *Progress in*
573 *Polymer Science, 37*(12), 1678-1719.

574 Cal, P.M., Frade, R.F.M., Chudasama, V., Cordeiro, C., Caddick, S. & Gois, P.M.P. (2014)
575 Targeting cancer cells with folic acid–iminoboronate fluorescent conjugates. *Chemical*
576 *Communications, 50,* 5261-5263.
577 Canton, E., Peman, J., Gobernado, M., Viudes, A. & Espinel-Ingroff A. (2004) Patterns of
578 Amphotericin B Killing Kinetics against Seven *Candida* Species. *Antimicrobial Agents*
579 *Chemotherapy*, *48(7)*, 2477-2482.
580 Carreau, P. J. (1972) Rheological Equations from Molecular Network Theories. *Journal of*
581 *Rheology*, *16*(1), 99-127.
582 Chawla, P., Ranjan Srivastava, A., Pandey, P. & Chawla, V. (2014**)** Hydrogels: A journey
583 from diapers to gene delivery. *Mini-reviews in Medicinal Chemistry, 14*(2*)*, 154-167.
584 De Seta, F., Schmidt, M., Vu, B., Essmann, M. & Larsen, B. (2009) Antifungal mechanisms
585 supporting boric acid therapy of *Candida* vaginitis. *Journal of Antimicrobial*
586 *Chemotherapy*, *63*(2), 325-336.
587 Dinu, M. V., Pradny, M., Dragan, E. S. & Michalek, J. (2013) Ice-templating hydrogels based
588 on chitosan with tailored porous morphology, *Carbohydrate Polymers 94*(1), 170-178.
589 Ebara, M., Kotsuchibashi, Y., Narain, R., Idota, N., Kim, Y.Y., Hoffman, J.M., Uto, K.,
590 Aoyagi, T., *Smart Hydrogels* in *Smart Biomaterials*, Springer Japan, 2014, 9-65.
591 Fajardo, A.A., Favaro, S.L., Rubira A. F & Muniz, E.C. (2013) Dual-network hydrogels
592 based on chemically and physically crosslinked chitosan/chondroitin sulfate. *Reactive &*
593 *Functional Polymers*, *73*(12), 1662-1671.

Gutiérrez-Moreno, N.J., Medrano, F. & Yatsimirsky, A.K. (2012) Schiff base formation and recognition of amino sugars, aminoglycosidesand biological polyamines by 2-formyl phenylboronic acid in aqueous solution. *Organic and Biomolecular Chemistry*, *10*, 6960-6972.

Hutin, M., Bernardinelli, G. & Nitschke, J. R. **(**2008) An Iminoboronate Construction Set for Subcomponent Self-Assembly. *Chemistry - A European Journal*, *14*(15), 4585-4593.

Kumar, M.N., Muzzarelli, R.A., Muzzarelli, C., Sashiwa H. & Domb A.J. (2004) Chitosan chemistry and pharmaceutical perspectives, *Chemical Reviews*, *104*(12),6017-6084.

Leceta, I., Guerrero, P., Ibarburu, I., Dueñas, M. T., de la Caba, K. (2013) Characterization and antimicrobial analysis of chitosan-based films. *Journal of Food Engineering. 116*(4), 889-899.

Lee, L.Z.A, Ng, W.L.V., Lee Poon, G., Ke, X., Hedrick, J.L. & Yang, Y.Y. (2015). Co-delivery of antiviral and antifungal therapeutics for the treatment of sexually transmitted infections using a moldable, supramolecular hydrogel. *Advanced Healthcare Materials*, *4*, 385-394.

Mahkam M. (2010). Modified chitosan cross-linked starch polymers for oral insulin delivery, *Journal of Bioactive and Compatible Polymers*, *25*, 406-418.

Marin, L., Ailincai, D., Mares, M., Paslaru, E., Cristea, M., Nica, V. & Simionescu, B.C. (2015) Imino-chitosan biopolymeric films. Obtaining, self-assembling, surface and antimicrobial properties. *Carbohydrate Polymers*, *117*, 762-770.

Marin, L., Morariu, S., Popescu, M.-C., Nicolescu, A., Zgardan, C. Simionescu, B. C. Barboiu, M. (2014), Out-of-Water Constitutional Self-Organization of Chitosan–Cinnamaldehyde Dynagels. *Chemistry - A European Journal*, *20*(16), 4814–4821.

617 Marin, L., Simionescu, B. C. & Barboiu M. (2012) Imino-chitosan biodynamers. *Chemical*
618 *Communications*, *48*, 8778–8780.
619 Marin, L., Stoica, I., Mares, M., Dinu, V., Simionescu, B.C. & Barboiu, M. (2013)
620 Antifungal vanillin-imino-chitosan biodynameric films. *Journal of Materials Chemistry B*.
621 *1*, 3353-3358.
622 Marin, L., Damaceanu, M. D. & Timpu D. (2009) New thermotropic liquid crystalline
623 polyazomethines containing luminescent mesogens. *Soft Materials, 7*(1), 1-20.
624 Marques, M.R.C., Loebenberg, R. & Almukainzi, M. Simulated biological fluids with
625 possible application in dissolution testing. *Dissolution Technologies*, 2011, *18(3)*, 15-28.
626 Mi, F. L., Kuan, C. Y., Shyu, S. S., Lee, S. T. & Chang, S. F. (2000) Study of gelation
627 kinetics and chain-relaxation properties of glutaraldehyde-cross-linked chitosan gel and
628 their effects on microspheres preparation and drug release. *Carbohydrate Polymers, 41*(4),
629 389-396.
630 Mikhailov, S.N., Zakharova, A.N., Drenichev, M.S., Ershov, A.V., Kasatkina, M.A.,
631 Vladimirov, L.V., Novikov V.V. & Kildeeva N.R. (2016). Crosslinking of chitosan with
632 dialdehyde derivatives of nucleosides and nucleotides. Mechanism and comparison with
633 glutaraldehyde. *Nucleosides, nucleotides and nucleic acids*.
634 10.1080/15257770.2015.1114132.
635 Moosa, M.-Y., Sobel, J.D., Elhalis, H., Du W. & Akins R.A. (2004) Fungicidal activity of
636 fluconazole against *Candida albicans* in a synthetic vagina-simulative medium
637 *Antimicrobrial Agents and Chemotherapy, 48*(1), 161-167.
638 Muzzarelli, R.A.A., Ilari, P., Xia, W., Pinotti, M., & Tomasetti, M. (1994). Tyrosinase-
639 mediated quinone tanning of chitinous materials. *Carbohydrate Polymers, 24*, 294-300.

Palumbo, F.S., Fiorica, C., Di Stefano, M., Pitarresi, G., Gulino, A., Agnello, S. & Giammona, G. (2015**)** In situ forming hydrogels of hyaluronic acid and inulin derivatives for cartilage regeneration. *Carbohydrate Polymers, 122*, 408-416.

Pasa, S., Aydın, S., Kalaycı, S., Boğa, M., Atlan, M., Bingul, M., Şahin, F., Temel, H. (2016) The synthesis of boronic-imine structured compounds and identification of their anticancer, antimicrobial and antioxidant activities. *Journal of Pharmaceutical Analysis*, *6*, 39–48.

Pierce, C. G., Uppuluri, P., Tristan, A. R., Wormley Jr., F. L., Mowat, E., Ramage, G. & Lopez-Ribot, J.L. (2008) A simple and reproducible 96-well plate-based method for the formation of fungal biofilms and its application to antifungal susceptibility testing. *Nature Protocols*, *3*(9), 1494-1500.

Ravi Kumar, M.N.V., Muzzarelli, R.A.A., Muzzarelli, C., Sashiwa, H. & Domb, A.J. (2004) Chitosan chemistry and pharmaceutical perspectives. *Chemical Reviews, 104*, 6017-6084.

Sobel, J. D. (2016) Recurrent vulvovaginal candidiasis. *American Journal of Obstetrics and Gynecology*, *214*(1), 115-121.

Ullah, F., Bisyrul, M., Othman, H., Javed, F., Ahmad, Z. & Akil, H. (2015) Classification, processing and application of hydrogels: A review. *Materials Science & Engineering C-Materials for Biological Applications C, 57*, 414-433.